Interaction-enhanced altermagnet in the Hatsugai-Kohmoto model

Ádám Bácsi [1,2,*] and Balázs Dóra [3,2,†]

[1] *Department of Mathematics and Physics, Széchenyi István University, 9026 Győr, Hungary*

[2] *MTA-BME Lendület "Momentum" Open Quantum Systems Research Group, Institute of Physics, Budapest University of Technology and Economics, Műegyetem rkp. 3, H-1111 Budapest, Hungary*

[3] *Department of Theoretical Physics, Institute of Physics, Budapest University of Technology and Economics, Műegyetem rkp. 3, H-1111 Budapest, Hungary*

(Received 17 November 2025; accepted 13 May 2026; published 26 May 2026)

We investigate the interplay between altermagnetic band structures and electronic correlations by focusing on the $d_{x^2-y^2}$ altermagnetic generalization of the Hatsugai-Kohmoto model. We find that with increasing interaction, a many-body Lifshitz transition takes place when doubly occupied regions disappear from the Fermi surface and almost all momentum states become fully spin polarized. This is termed interaction-enhanced altermagnet. We find that the dynamical susceptibility, which possesses only transverse nonzero components for small wave vectors, develops a gap proportional to the interaction strength and displays a sharp peak at a frequency increasing with the interaction. Above the Lifshitz transition, this peak moves to the lower gap edge and becomes log divergent. The signal intensity increases with the interaction up until the Lifshitz transition and saturates afterward. The static susceptibility remains unaffected by the correlations and altermagnetism reduces the static transverse response.

DOI: 10.1103/p54n-mvb8

I. INTRODUCTION

Altermagnets are a recently discovered class of magnetic materials [1–15] characterized by simultaneous breaking of certain crystal symmetries and time-reversal symmetry. The net magnetization of these materials is zero just like in antiferromagnets but they have a peculiar, spin-dependent band structure that is more typical to ferromagnets. The signatures of altermagnetism are observable in numerous physical quantities such as the optical conductivity [6] or angle-resolved spectroscopy measurements [11,16] revealing significant spin dependence of the band structure. Further experimental evidence comes from magneto-optical Kerr responses [17] and anisotropic magnetoresistance [18], as well as from magnon transport measurements [19], all indicating robust spin polarization without macroscopic magnetization. Due to their spin-dependent fermionic excitations, they are promising candidates for information technology and spintronical applications.

From a theoretical perspective, altermagnetism arises from the interplay between collinear antiferromagnetic order and crystal symmetries, leading to alternating spin polarization in momentum space [1,20]. This effect leads to a description in terms of noninteracting fermionic excitations

*Contact author: bacsi.adam@sze.hu

†Contact author: dora.balazs@ttk.bme.hu

Published by the American Physical Society under the terms of the Creative Commons Attribution 4.0 International license. Further distribution of this work must maintain attribution to the author(s) and the published article's title, journal citation, and DOI.

with spin-dependent energy spectra. While this single-particle picture captures the essential band features, the role of electronic correlations on top of altermagnetism remains largely unexplored [7,21]. Strong interactions often yield to a variety of peculiar phenomena, ranging from Mott insulating behavior and phase transitions to non-Fermi liquid and pseudogap physics [22–25]. A natural way to incorporate interactions into a tractable theoretical framework is provided by the Hatsugai-Kohmoto (HK) interaction [26–33], which combines a transparent physical picture with analytical solvability and which is at the same time a prototypical example of non-Fermi liquids [34]. In addition, the HK model [35] can be continuously deformed to the Hubbard model by systematically introducing momentum mixing, going from qualitative to quantitative agreement between these models.

Here, we focus on the effect of strong correlations in an altermagnet. We employ a direct evaluation of the Kubo formula [36,37] by explicitly incorporating many-body occupation probabilities, which represents a natural framework to study the response functions of the HK model. This is in contrast to the conventional treatment based on single-particle Green's function and single-particle occupation probabilities. Therefore, our approach provides a more intuitive and suitable basis to analyze the interplay between altermagnetism and the HK interaction.

We identify rich physics, including a many-body Lifshitz transition due to correlations, when momentum space doublons are excluded from the Fermi surface and almost all momentum states become fully spin polarized. This results in interaction-enhanced altermagnetism. This is also reflected in the dynamical spin response. It displays an interaction-induced gap and a sharp peak, which becomes divergent above the Lifshitz transition. In this regime, the signal intensity remains constant in the interaction-enhanced altermagnetic phase due to the frozen and spin-polarized Fermi surface without doublons; only its lower gap edge moves to higher frequencies with increasing interaction. In spite of the strong interaction dependence of the dynamical susceptibility, the static Pauli response remains independent from correlations and is only influenced by the altermagnetic band structure.

II. ALTERMAGNET WITH HATSUGAI-KOHMOTO INTERACTION

Altermagnets are known for their spin-dependent energy spectra as a consequence of lifted Kramers spin degeneracy [8]. In this paper, we study the interplay between the spin dependence of a two-dimensional altermagnet and the HK interaction describing a local interaction in momentum space. The Hamiltonian of the system reads

$$H = \sum_{\mathbf{k}s} \varepsilon_s(\mathbf{k}) c^+_{\mathbf{k}s} c_{\mathbf{k}s} + \sum_{\mathbf{k}} U n_{\mathbf{k}\uparrow} n_{\mathbf{k}\downarrow}, \tag{1}$$

where the spin-dependent energy spectrum

$$\varepsilon_\uparrow(\mathbf{k}) = \frac{k_x^2}{2m}\alpha + \frac{k_y^2}{2m}\frac{1}{\alpha}, \quad \varepsilon_\downarrow(\mathbf{k}) = \frac{k_x^2}{2m}\frac{1}{\alpha} + \frac{k_y^2}{2m}\alpha \tag{2}$$

describes the $d_{x^2-y^2}$ altermagnetism with α measuring the asymmetry between band structures of the opposite spin directions ($\alpha = 1$ corresponds to the symmetric case). We also note that our results also apply to altermagnets with d_{xy} symmetry. The energy spectrum (2) describes the effective low-energy model expanded to quadratic order in momenta around the spin-degeneracy points (Brillouin zone center) of systems obeying combined time-reversal and fourfold rotation symmetry, a typical feature in altermagnets [2,6,8].

In the second term of Eq. (1), U measures the strength of the HK interaction [26,27] and $n_{\mathbf{k}s} = c^+_{\mathbf{k}s} c_{\mathbf{k}s}$, with $c_{\mathbf{k}s}$ the annihilation operator of electrons and we use $\hbar = 1$.

Note that the system breaks both the time-reversal T and the rotation symmetry but preserves C_4T, the combination of a fourfold rotation and time reversal [6].

We comment on the physical relevance of our model in Eq. (1), which is deceivingly simple and contains a contact interaction in momentum space, which translates to a long-range interaction

in real space [26]. While this is hardly realized in physical systems, the ensuing physics of our model is expected to describe qualitatively the behavior of strongly correlated altermagnets. In addition to the altermagnetic band structure, the interaction term penalizes double occupancies, which is the general behavior of Hubbard-type models. Moreover, the HK model [35] was shown to be continuously connected to the Hubbard model by introducing momentum mixing terms in the interaction, resulting in quantitative agreement between these models. Consequently, the HK model provides at least a qualitative description of Hubbard-type physics.

As to possible other phases, the low-energy spectrum in Eq. (2) applies to low fillings on tight-binding models [6], away from Fermi surface nesting conditions. Therefore, no additional phases are expected for repulsive interactions [38], except for the possible Mottness. Close to commensurate fillings, additional phases (e.g., antiferromagnetic) could be possible, which is beyond the scope of our model and investigation.

The great advantage of the HK model is that the Hamiltonian decouples to different wave number sectors characterized by four many-body basis states of $|\mathbf{k}, 0\rangle$, $|\mathbf{k}, \uparrow\rangle$, $|\mathbf{k}, \downarrow\rangle$, and $|\mathbf{k}, \uparrow\downarrow\rangle$. These describe states with no electron, only spin-up occupancy, only spin-down occupancy, or double occupancy in the mode $\mathbf{k}$, respectively. The density matrix at thermal equilibrium is diagonal in this basis with the entries of the following many-body occupation probabilities:

$$\begin{aligned} P(\mathbf{k}, 0) &= \langle (1 - n_{\mathbf{k}\uparrow})(1 - n_{\mathbf{k}\downarrow}) \rangle = \frac{1}{Z_{\mathbf{k}}}, \\ P(\mathbf{k}, s) &= \langle n_{\mathbf{k}s}(1 - n_{\mathbf{k}\bar{s}}) \rangle = \frac{e^{-\beta \xi_s(\mathbf{k})}}{Z_{\mathbf{k}}}, \\ P(\mathbf{k}, \uparrow\downarrow) &= \langle n_{\mathbf{k}\uparrow} n_{\mathbf{k}\downarrow} \rangle = \frac{e^{-\beta(\xi_\uparrow(\mathbf{k}) + \xi_\downarrow(\mathbf{k}) + U)}}{Z_{\mathbf{k}}}, \end{aligned} \tag{3}$$

with $\bar{s} = -s$ and

$$Z_{\mathbf{k}} = 1 + e^{-\beta \xi_\uparrow(\mathbf{k})} + e^{-\beta \xi_\downarrow(\mathbf{k})} + e^{-\beta(\xi_\uparrow(\mathbf{k}) + \xi_\downarrow(\mathbf{k}) + U)} \tag{4}$$

the partition function corresponding to the momentum channel $\mathbf{k}$, $\xi_s(\mathbf{k}) = \varepsilon_s(\mathbf{k}) - \mu$, and β is the inverse temperature. The probabilities $P(\mathbf{k}, \sqcup)$ are the many-body counterparts of the products of occupation numbers in a typical noninteracting situation. In fact, when $U = 0$, these occupation probabilities boil down to simple products with the Fermi function. For example, $P(\mathbf{k}, \uparrow) = f(\xi_\uparrow(\mathbf{k}))(1 - f(\xi_\downarrow(\mathbf{k})))$ for $U = 0$.

Let us now examine the ground state of the system assuming that the electronic spectrum is filled up to the chemical potential μ. In the ground state, the many-body occupation probabilities become either one, for the lowest energy many-body state, or zero, for the other states. In the noninteracting case, $U = 0$, Fig. 1(a) shows the $\mathbf{k}$ dependence of the spin configuration realized in the ground state. The Fermi surface consists of two, intersecting ellipses corresponding to the two spin orientations. The peculiarity of the altermagnetic electron spectrum is that the ground state includes singly occupied regions with well-defined spin polarization; see the blue and red regions in Fig. 1(a).

In the presence of finite interaction strength U, the double occupancy is suppressed at fixed chemical potential [see Fig. 1(b)]. The size of singly occupied, spin-polarized regions grows; therefore, altermagnetic features are expected to be enhanced by increasing the interaction U. This can be called an *interaction-enhanced altermagnet*. We note that this is not an emergent structure but rather follows from the interplay of the original altermagnetic band dispersion and interaction.

At fixed number of electrons, a U-dependent chemical potential emerges as

$$\mu(U) = \begin{cases} \left(1 - \frac{U}{U_c}\right)\mu_0 + U, & \text{for } U < U_c, \\ U_c, & \text{for } U > U_c, \end{cases} \tag{5}$$

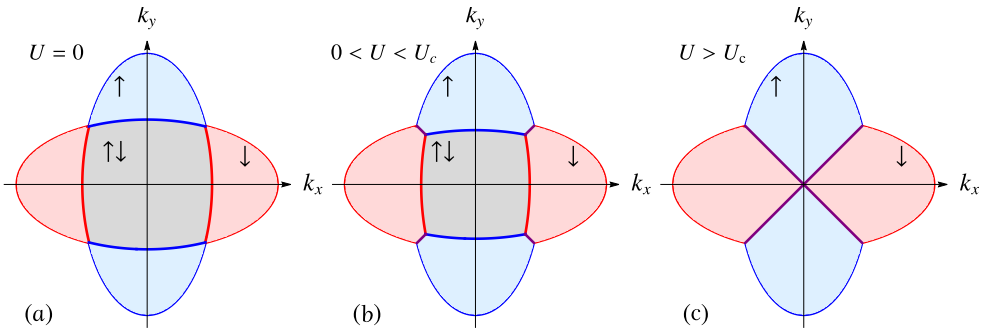


FIG. 1. Schematic picture of the ground-state occupation of many-body states as a function of momentum in (a) the noninteracting ($U = 0$), (b) moderately interacting ($0 < U < U_c$), and (c) strongly interacting ($U > U_c$) cases. In the blue region, the up spin state is occupied while the down spin state is empty. In the red region, only the down spin state is occupied. The gray area indicates double occupancy. Panel (c) can be termed "interaction-enhanced altermagnet" due to the lack of double occupancies and fully polarized momentum states.

where $\mu_0 = \frac{\pi n_e}{m}$ is the chemical potential at $U = 0$ corresponding to the electron density n_e and $U_c = \mu_0(1 - B(\alpha))^{-1}$, with $B(\alpha) = \frac{2}{\pi}\arctan(\min(\alpha, \alpha^{-1}))$. Here, U_c denotes the critical interaction strength above which no double occupancy is present for a given number of particles in the ground state and each momentum state is spin polarized except for the momenta along the degeneracy curves at the border of the spin-up and spin-down regions that, however, constitute a zero-measure set in the momentum space; therefore, the system is almost everywhere spin polarized. This we will refer to as fully spin-polarized state and it is shown in Fig. 1(c). The exclusion of double occupancies in the Fermi surface indicates a many-body Lifshitz transition [39,40] at U_c. In the $U > U_c$ region, there still exist gapless excitations, but the system exhibits Mott insulator features in the sense that the shape of the Fermi surface does not change with further increase of U [26] and optical excitations do not probe the gapless modes. Hence, this regime can be regarded as an effective Mott insulating altermagnet. A real Mott insulator without additional gapless modes is expected to emerge at specific fillings beyond the low-energy model, when the interaction strength becomes comparable to the bandwidth.

The Lifshitz transition is not a typical weak-coupling instability because its critical interaction range is $\mu_0 < U_c < 2\mu_0$ depending on the value of α. This is further corroborated by evaluating the density of particles in doublonic configuration in the ground state from

$$n_{\uparrow\downarrow} = \frac{2}{A}\sum_k P(\mathbf{k}, \uparrow\downarrow) = 2n_e\left(1 - \frac{U}{U_c}\right)B(\alpha), \tag{6}$$

when $U < U_c$ and zero for $U > U_c$, and A is the area of the system. For $U = 0$ and $\alpha = 1$, the ground state consists of momentum space doublons and $n_{\uparrow\downarrow} = n_e$.

The analysis of the ground state shows that the HK interaction reorganizes the Fermi surface and, in turn, the structure of occupation probabilities, which is dominated by many-body features. In the following sections, we study how these correlation effects influence the linear response of the system.

III. SPIN SUSCEPTIBILITY TENSOR

The unique signature of altermagnets is their peculiar spin-dependent band structure in Fig. 1. The best way to directly probe and reveal this is to study spin-dependent quantities, such as the spin response. To this end, we analyze the full 3×3 spin susceptibility tensor, which is defined by the

Kubo formula as

$$\chi_{nm}(\mathbf{R},t) = i\mu_B^2\langle[\hat{S}^n(\mathbf{R},t),\hat{S}^m(0,0)]\rangle \tag{7}$$

for positive times and 0 for negative t. The indices n and m stand for the spin components x, y, or z, μ_B is the Bohr magneton, and $\mathbf{R}$ is the two-dimensional space variable. The spin operators are expressed with the fermionic operators as

$$\hat{S}^n(\mathbf{R},t) = \frac{1}{N}\sum_{\mathbf{k}\mathbf{k}',ss'} e^{i(\mathbf{k}-\mathbf{k}')\mathbf{R}} c^+_{\mathbf{k}s}(t)\sigma^n_{ss'}c_{\mathbf{k}'s'}(t), \tag{8}$$

with σ^n denoting the Pauli matrices and N the number of unit cells. After some algebraic steps, detailed in the Appendix, we obtain

$$\begin{aligned}\chi_{nm}(\mathbf{q},\omega) = \lim_{\delta\to 0^+}\int_0^\infty e^{i\omega t-\delta t}\chi(\mathbf{q},t)\,\mathrm{d}t &= -\frac{\mu_B^2}{N}\delta_{\mathbf{q},0}\sum_{\mathbf{k},s}\sigma^n_{s\bar{s}}\sigma^m_{\bar{s}s}\frac{P(\mathbf{k},s)-P(\mathbf{k},\bar{s})}{\omega+i\delta+\varepsilon_s(\mathbf{k})-\varepsilon_{\bar{s}}(\mathbf{k})}\\
&-\frac{\mu_B^2}{N}(1-\delta_{\mathbf{q},0})\sum_{\mathbf{k},ss'}\sigma^n_{ss'}\sigma^m_{s's}\Bigg[\frac{P(\mathbf{k}+\mathbf{q},s)P(\mathbf{k},0)-P(\mathbf{k}+\mathbf{q},0)P(\mathbf{k},s')}{\omega+i\delta+\varepsilon_s(\mathbf{k}+\mathbf{q})-\varepsilon_{s'}(\mathbf{k})}\\
&+\frac{P(\mathbf{k}+\mathbf{q},\uparrow\downarrow)P(\mathbf{k},0)-P(\mathbf{k}+\mathbf{q},\bar{s})P(\mathbf{k},s')}{\omega+i\delta+\varepsilon_s(\mathbf{k}+\mathbf{q})-\varepsilon_{s'}(\mathbf{k})+U}\\
&+\frac{P(\mathbf{k}+\mathbf{q},s)P(\mathbf{k},\bar{s}')-P(\mathbf{k}+\mathbf{q},0)P(\mathbf{k},\uparrow\downarrow)}{\omega+i\delta+\varepsilon_s(\mathbf{k}+\mathbf{q})-\varepsilon_{s'}(\mathbf{k})-U}\\
&+\frac{P(\mathbf{k}+\mathbf{q},\uparrow\downarrow)P(\mathbf{k},\bar{s}')-P(\mathbf{k}+\mathbf{q},\bar{s})P(\mathbf{k},\uparrow\downarrow)}{\omega+i\delta+\varepsilon_s(\mathbf{k}+\mathbf{q})-\varepsilon_{s'}(\mathbf{k})}\Bigg],\end{aligned} \tag{9}$$

which is the most general form of the spin susceptibility tensor for a system with $\mathbf{k}$-diagonal many-body occupation probabilities.

The first term in the susceptibility corresponds to the exact zero wave number, $\mathbf{q}=0$. However, this contribution is physically not relevant because all excitations, including optical excitations, possess a nonzero wave number. Therefore, this term will be neglected in the following sections similarly to Ref. [30]. We note that, due to the properties of the Pauli matrices, the tensor elements χ_{xz}, χ_{zx}, χ_{yz}, and χ_{zy} vanish. The remaining tensor elements will be studied in specific cases.

IV. DYNAMICAL SPIN SUSCEPTIBILITY

We consider the homogeneous limit, $\mathbf{q}\to 0$, while keeping ω finite. This is relevant experimentally in condensed matter [41] for neutron [42,43] as well as x-ray scattering, electron spin resonance studies [44–46], and for cold atoms using spin-dependent Bragg spectroscopy [47].

We focus on zero temperature such that the probabilities $P(\mathbf{k},\sqcup)$ take values of 1 inside certain regions of the momentum space and 0 outside. This significantly simplifies Eq. (9), as the products $P(\mathbf{k},\sqcup)P(\mathbf{k},\sqcup')$ vanish whenever $\sqcup$ and $\sqcup'$ are different as these are mutually exclusive events or probabilities. As a consequence, the tensor element $\chi_{zz}(\omega)$ is identically zero. The remaining components are expressed as

$$\begin{aligned}\chi_{xx}(\omega) = \chi_{yy}(\omega) &= \Gamma_{\uparrow\downarrow}(\omega)+\Gamma_{\downarrow\uparrow}(\omega),\\
\chi_{xy}(\omega) = -\chi_{yx}(\omega) &= i(\Gamma_{\uparrow\downarrow}(\omega)-\Gamma_{\downarrow\uparrow}(\omega)),\end{aligned} \tag{10}$$

where

$$\Gamma_{\uparrow\downarrow}(\omega) = \frac{\mu_B^2}{N}\lim_{\delta\to 0^+}\sum_{\mathbf{k}}\left[\frac{P(\mathbf{k},\uparrow)^2}{\omega+i\delta+\varepsilon_\downarrow(\mathbf{k})-\varepsilon_\uparrow(\mathbf{k})+U}-\frac{P(\mathbf{k},\downarrow)^2}{\omega+i\delta+\varepsilon_\downarrow(\mathbf{k})-\varepsilon_\uparrow(\mathbf{k})-U}\right], \tag{11}$$

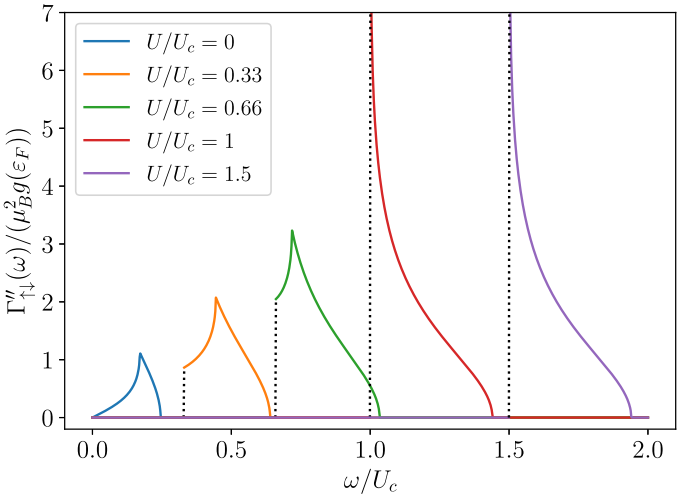


FIG. 2. Frequency dependence of the dynamical spin susceptibility is shown at $\alpha = 1.2$ for various values of U and $\mu_0 = (1 - B(1.2))U_c$.

and $\Gamma_{\downarrow\uparrow}(\omega) = (\Gamma_{\uparrow\downarrow}(-\omega))^*$ are the spin-flip response functions. The nonvanishing terms in $\Gamma_{\uparrow\downarrow}(\omega)$ can be associated with specific spin-flip processes. The first term with $P(\mathbf{k}, \uparrow)^2$ corresponds to the situation where two spin-up particles occupy states at $\mathbf{k}$ and infinitesimally close to $\mathbf{k}$ within the blue region of Fig. 1(b). In this region, the spin-down state is unoccupied, allowing the spin-flip process resulting in double occupancy at $\mathbf{k}$. Similarly, the second term $P(\mathbf{k}, \downarrow)^2$ corresponds to a spin-flip process involving spin-down particles in the red region of Fig. 1(b).

After taking the limit $\delta \to 0^+$, two kinds of terms appear in the response function, $\Gamma_{\uparrow\downarrow}(\omega) = \Gamma'_{\uparrow\downarrow}(\omega) + i\Gamma''_{\uparrow\downarrow}(\omega)$. Here, Γ' includes the terms with the principal value functions and Γ'' includes the Dirac-delta terms. Note that Γ' and Γ'' are related to each other by Kramers-Kronig relations. Henceforth, we focus on Γ'' only.

The frequency dependence is analytically obtained as

$$\Gamma''_{\uparrow\downarrow}(\omega) = \frac{\mu_B^2 g(\varepsilon_F)}{\alpha - \alpha^{-1}} \begin{cases} \operatorname{artanh}\sqrt{\frac{(\alpha^2-1)\mu-(\omega-U)}{(\alpha^2-1)\mu+\alpha^2(\omega-U)}} - \operatorname{artanh}\sqrt{\frac{(\alpha^2-1)(\mu-U)-\alpha^2(\omega-U)}{(\alpha^2-1)(\mu-U)+(\omega-U)}}, & \text{for } U < \omega < \omega_m, \\ \operatorname{artanh}\sqrt{\frac{(\alpha^2-1)\mu-(\omega-U)}{(\alpha^2-1)\mu+\alpha^2(\omega-U)}}, & \text{for } \omega_m < \omega < \alpha^2\omega_m, \end{cases} \tag{12}$$

and 0 otherwise for $\omega > 0$ and $\Gamma''_{\uparrow\downarrow}(-\omega) = -\Gamma''_{\uparrow\downarrow}(\omega)$ for the negative frequencies. In Eq. (12),

$$\omega_m = U + \left(1 - \frac{1}{\alpha^2}\right)(\mu - U) \tag{13}$$

denotes the location of the peak with the most intense spin-flip response and $g(\varepsilon_F) = \frac{A_c m}{\pi}$ is the total density of states of the noninteracting electrons, with $A_c = A/N$ the area of the unit cell and includes both spin directions. It is also energy and α independent. Equations (12) and (13) are valid for $\alpha > 1$, and for $\alpha < 1$, α should be replaced by α^{-1}.

Due to the oddness of $\Gamma''_{\uparrow\downarrow}(\omega)$, the tensor elements $\chi''_{xy}(\omega)$ and $\chi''_{yx}(\omega) = 0$ vanish, while $\chi''_{xx}(\omega) = \chi''_{yy}(\omega) = 2\Gamma''_{\uparrow\downarrow}(\omega)$. The frequency dependence of $\Gamma''_{\uparrow\downarrow}$ is plotted in Fig. 2.

The spin susceptibility develops a gap of U at finite interaction strength. This is the energy cost of forming a $\uparrow\downarrow$ pair from two spin-up particles located infinitesimally close to each other through the spin-flip process. Figure 2 shows that increasing interaction strength enhances the signal intensity of the dynamical spin susceptibility, which also originates from the enlarged spin-polarized regions

in the momentum space from Fig. 1. The maximum response at ω_m is found as

$$\Gamma''_{\uparrow\downarrow,\max} = \frac{\mu_B^2 g(\varepsilon_F)}{\alpha - \alpha^{-1}} \operatorname{artanh}\left(\sqrt{\frac{\mu(\alpha^2-1)+U}{\alpha^2(2\mu - U)}}\right). \tag{14}$$

As the interaction strength approaches U_c, the maximum location shifts to the lower gap edge $\omega_m = U$ and the maximum value [Eq. (14)] diverges logarithmically.

Beyond the Lifshitz transition, $U > U_c$, the frequency dependence has the same structure as at U_c with a log divergent peak at the lower gap edge as $\sim -\ln(\omega - U)$. This arises from a saddle point in momentum space from the denominator of Eq. (11) since $\varepsilon_\uparrow(\mathbf{k}) - \varepsilon_\downarrow(\mathbf{k}) \sim k_x^2 - k_y^2$.

The dynamical susceptibility above the Lifshitz transition is described by the second row of Eq. (12) with $\mu = U_c$ and is located between $U < \omega < U + (\alpha^2 - 1)U_c$. Hence, the shape of the response function remains essentially unchanged. Further increasing the interaction strength only shifts the response function toward higher frequencies, reflecting the growing separation between the lower and upper Hubbard bands. The shape of the Fermi surface does not change any more in Fig. 1 as doublons are already excluded from it. Similar features are expected to occur in an altermagnetic Mott insulators beyond the transition point. There, the lower Hubbard band is completely filled [26] without doublons and is separated by a clean gap from the upper Hubbard band. Although our lower Hubbard band is only partially filled in this case, small momentum optical excitations only allow for vertical transitions and cannot reveal the partial filling of the lower band. Therefore, the $U > U_c$ small momentum spin response is analogous in this respect to that of an altermagnetic Mott insulator.

Finally, we comment on the nature of gapped spin excitations in an otherwise gapless system. The linear shift of the resonance peak upon increasing interaction strength may be model dependent but the gap opening is expected on general ground due to the extra energy associated with double occupancies from the interaction.

V. STATIC SUSCEPTIBILITY

In this section, we analyze the static susceptibility, $\omega = 0$, in the homogeneous limit, $\mathbf{q} \to 0$. In contrast to the dynamical susceptibility, the zz component of the static response function remains finite at zero temperature. Interestingly, this component is independent of the interaction strength U and the asymmetry parameter α, and is given by

$$\chi_{zz}^{\mathrm{st}} = \mu_B^2 g(\varepsilon_F), \tag{15}$$

which is the conventional Pauli susceptibility [48].

The remaining, nonvanishing components of the susceptibility tensor are calculated as

$$\chi_{xx}^{\mathrm{st}} = \chi_{yy}^{\mathrm{st}} = \chi_{zz}^{\mathrm{st}} C(\alpha, U), \tag{16}$$

with

$$C(\alpha, U) = \frac{4}{\pi}\int_{\pi/4}^{\pi/2} \frac{\mathrm{d}\varphi}{v(\varphi)} \ln\left(\frac{\frac{U}{\mu} + \frac{2v(\varphi)}{\alpha + \frac{1}{\alpha} - v(\varphi)}}{\frac{U}{\mu} + \frac{2\left(1-\frac{U}{\mu}\right)v(\varphi)}{\alpha + \frac{1}{\alpha} + v(\varphi)}}\right), \tag{17}$$

where $v(\varphi) = \cos(2\varphi)(\frac{1}{\alpha} - \alpha)$. After some algebraic steps, it can be shown that the integral is independent of the interaction strength U. This independence is related to the fact that contributions to the static susceptibility dominantly come from intraband processes. Since the finite interaction only splits the band structure to upper and lower Hubbard bands [26] and does not alter its shape, the characteristics of intraband processes are expected to be preserved at finite interaction strength.

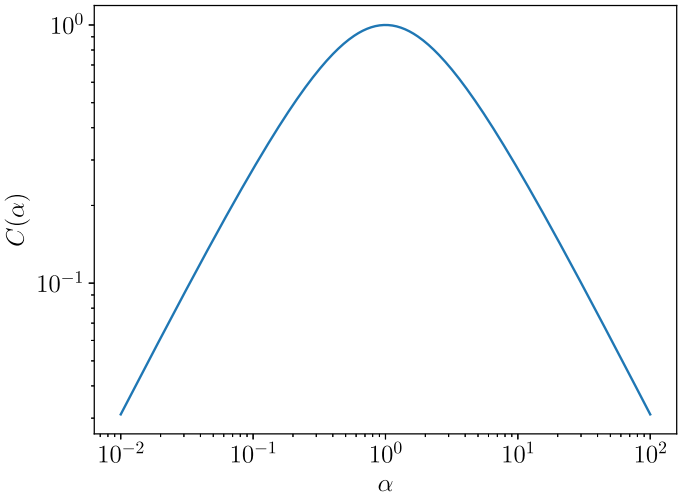


FIG. 3. $C(\alpha)$ is plotted for the α dependence of the transverse static spin susceptibility, which is symmetric for $\alpha \leftrightarrow 1/\alpha$ change from Eq. (18).

The U-independent integral

$$C(\alpha) = \frac{4}{\pi} \int_{\pi/4}^{\pi/2} \frac{\mathrm{d}\varphi}{v(\varphi)} \ln\left(\frac{\alpha + \frac{1}{\alpha} + v(\varphi)}{\alpha + \frac{1}{\alpha} - v(\varphi)}\right) \tag{18}$$

is computed numerically and is symmetric under $\alpha \leftrightarrow 1/\alpha$. The results shown in Fig. 3 indicate that the asymmetry parameter α suppresses the susceptibility as moving away from the symmetrical point $\alpha = 1$. In particular, $C(\alpha \to \infty) \to \pi/\alpha$.

VI. DISCUSSION

We have analyzed the interplay between altermagnetism and electronic correlations through the lens of the spin susceptibility. The electron-electron interaction has been modeled using the Hatsugai-Kohmoto model that enables analytically exact solutions. It serves as baseline model for non-Fermi liquids and Mottness and, by introducing proper momentum mixing, can also be continuously deformed to the Hubbard model [35]. The exact effects of the momentum-mixing terms on the spin response function need further investigations but qualitatively similar results are expected for the altermagnetic Hubbard model at low fillings. By studying a Hatsugai-Kohmoto altermagnet, we find that the noninteracting altermagnet undergoes a many-body Lifshitz transition with increasing interaction when momentum space doublons are completely excluded from the Fermi surface and almost all momentum states are fully spin polarized. The ensuing state is an interaction-enhanced altermagnet. The spin susceptibility is evaluated using the many-body occupation probabilities. The dynamical spin susceptibility develops a gap proportional to the interaction and initially displays a sharp though finite peak for larger frequencies.

Above the Lifshitz transition, this peak moves to the lower gap edge and becomes log divergent due to a momentum space saddle point. There, the Fermi surface remains intact and the shape of the dynamical spin susceptibility does not change further but acquires an overall shift to larger frequencies. Parallel to these, the signal intensity grows with interaction up until the transition and remains unchanged by further increasing the interaction.

The static, Pauli limit of the spin response is independent from the interaction strength though the transverse component gets altered by the altermagnetic band structure. Our results indicate how strong electronic correlations can enhance altermagnetism and reveal its fingerprints on dynamical spin probes.

ACKNOWLEDGMENTS

This work was supported by the National Research, Development and Innovation Office—NKFIH Projects No. K134437 and No. K142179, and by a grant of the Ministry of Research, Innovation and Digitization, CNCS/CCCDI-UEFISCDI, under Projects No. PN-IV-P1-PCE-2023-0159 and No. PN-IV-P1-PCE-2023-0987. This work was also supported by the HUN-REN Hungarian Research Network through the Supported Research Groups Programme, HUN-REN-BME-BCE Quantum Technology Research Group (TKCS-2024/34).

DATA AVAILABILITY

The data that support the findings of this article are openly available [49].

APPENDIX: ON THE DERIVATION OF EQ. (9)

Here, we discuss the explicit evaluation of the time-dependent Kubo formula for the Hatsugai-Kohmoto model. For Eq. (8), the time dependence of fermionic annihilation operators is obtained analytically as

$$c_{\mathbf{k}s}(t) = c_{\mathbf{k}s}e^{-i\varepsilon_s(\mathbf{k})t}\underbrace{(1-(1-e^{-iUt})n_{\mathbf{k}\bar{s}})}_{a_{\mathbf{k}\bar{s}}(t)}, \tag{A1}$$

where we introduced the operator $a_{\mathbf{k}\bar{s}}(t)$ involving the occupation number operator $n_{\mathbf{k}\bar{s}} = c^+_{\mathbf{k}\bar{s}}c_{\mathbf{k}\bar{s}}$. Note that neither $a_{\mathbf{k}\bar{s}}(t)$ nor $c_{\mathbf{k}s}(t)$ commute with $c_{\mathbf{k}\bar{s}}$. After substitution into the Kubo formula [Eq. (7)], we have

$$\begin{aligned}\chi_{nm}(\mathbf{R},t) = \frac{i\mu_B^2}{N^2}\sum_{\mathbf{k}\mathbf{k}',ss'}\sum_{\mathbf{k}_1\mathbf{k}'_1,s_1s'_1} e^{i(\mathbf{k}-\mathbf{k}')\mathbf{R}}e^{i(\varepsilon_s(\mathbf{k})-\varepsilon_{s'}(\mathbf{k}'))t} \\ \times \sigma^n_{ss'}\sigma^m_{s_1s'_1}\left\langle\left[c^+_{\mathbf{k}s}a_{\mathbf{k}\bar{s}}(t)^+a_{\mathbf{k}'\bar{s}'}(t)c_{\mathbf{k}'s'}, c^+_{\mathbf{k}_1s_1}c_{\mathbf{k}'_1s'_1}\right]\right\rangle,\end{aligned} \tag{A2}$$

where $\langle\rangle$ stands for the expectation value in thermal equilibrium. First, we evaluate the commutators and the expectation value. The operators a do not change the set of particles in a state. Therefore, the creation operators c^+ must be paired with the annihilation operators c in some order. Nonzero terms are proportional either to $\delta_{\mathbf{k}\mathbf{k}'}\delta_{ss'}\delta_{\mathbf{k}_1\mathbf{k}'_1}\delta_{s_1s'_1}$ or to $\delta_{\mathbf{k}\mathbf{k}'_1}\delta_{ss'_1}\delta_{\mathbf{k}_1\mathbf{k}'}\delta_{s_1s'}$. It can be shown that the $\delta_{\mathbf{k}\mathbf{k}'}\delta_{ss'}\delta_{\mathbf{k}_1\mathbf{k}'_1}\delta_{s_1s'_1}$ terms vanish. We substitute the remaining terms, which are proportional to $\delta_{\mathbf{k}\mathbf{k}'_1}\delta_{ss'_1}\delta_{\mathbf{k}_1\mathbf{k}'}\delta_{s_1s'}$, into the susceptibility and perform spatial Fourier transformation:

$$\chi_{nm}(\mathbf{q},t) = \sum_{\mathbf{R}} e^{-i\mathbf{q}\mathbf{R}}\chi_{nm}(\mathbf{R},t) = \frac{i\mu_B^2}{N}\sum_{\mathbf{k}\mathbf{k}',ss'}\delta_{\mathbf{k},\mathbf{k}'+\mathbf{q}}e^{i(\varepsilon_s(\mathbf{k})-\varepsilon_{s'}(\mathbf{k}'))t}\sigma^n_{ss'}\sigma^m_{s's}C_{\mathbf{k}\mathbf{k}',ss'}(t), \tag{A3}$$

where

$$\begin{aligned}C_{\mathbf{k}\mathbf{k}',ss'}(t) = \delta_{\mathbf{k}\mathbf{k}'}\delta_{s\bar{s}'}\langle n_{\mathbf{k}s}(1-n_{\mathbf{k}\bar{s}}) - (1-n_{\mathbf{k}s})n_{\mathbf{k}\bar{s}}\rangle + (1-\delta_{\mathbf{k}\mathbf{k}'})\langle a^+_{\mathbf{k}\bar{s}}(t)n_{\mathbf{k}s}\rangle\langle a_{\mathbf{k}'\bar{s}'}(t)(1-n_{\mathbf{k}'s'})\rangle \\ - (1-\delta_{\mathbf{k}\mathbf{k}'})\langle a^+_{\mathbf{k}\bar{s}}(t)(1-n_{\mathbf{k}s})\rangle\langle a_{\mathbf{k}'\bar{s}'}(t)n_{\mathbf{k}'s'}\rangle.\end{aligned} \tag{A4}$$

By using the probabilities $P(\mathbf{k},\sqcup)$ of Eq. (3), we obtain

$$\begin{aligned}C_{\mathbf{k}\mathbf{k}',ss'}(t) = \delta_{\mathbf{k}\mathbf{k}'}\delta_{s\bar{s}'}(P(\mathbf{k},s)-P(\mathbf{k},\bar{s})) + (1-\delta_{\mathbf{k}\mathbf{k}'})[e^{iUt}(P(\mathbf{k},\uparrow\downarrow)P(\mathbf{k}',0) - P(\mathbf{k},\bar{s})P(\mathbf{k}',s')) \\ + e^{-iUt}(P(\mathbf{k},s)P(\mathbf{k}',\bar{s}') - P(\mathbf{k},0)P(\mathbf{k}',\uparrow\downarrow)) + P(\mathbf{k},s)P(\mathbf{k}',0) + P(\mathbf{k},\uparrow\downarrow)P(\mathbf{k}',\bar{s}') \\ - P(\mathbf{k},0)P(\mathbf{k}',s') - P(\mathbf{k},\bar{s})P(\mathbf{k}',\uparrow\downarrow)].\end{aligned} \tag{A5}$$

We substitute into Eq. (A3) and perform the temporal Fourier transformation leading to Eq. (9).

[1] L. Šmejkal, J. Sinova, and T. Jungwirth, Beyond conventional ferromagnetism and antiferromagnetism: A phase with nonrelativistic spin and crystal rotation symmetry, Phys. Rev. X **12**, 031042 (2022).
[2] L. Šmejkal, J. Sinova, and T. Jungwirth, Emerging research landscape of altermagnetism, Phys. Rev. X **12**, 040501 (2022).
[3] S. Hayami, Y. Yanagi, and H. Kusunose, Momentum-dependent spin splitting by collinear antiferromagnetic ordering, J. Phys. Soc. Jpn. **88**, 123702 (2019).
[4] S. Hayami, Y. Yanagi, and H. Kusunose, Bottom-up design of spin-split and reshaped electronic band structures in antiferromagnets without spin-orbit coupling: Procedure on the basis of augmented multipoles, Phys. Rev. B **102**, 144441 (2020).
[5] Q. Cui, B. Zeng, P. Cui, T. Yu, and H. Yang, Efficient spin Seebeck and spin Nernst effects of magnons in altermagnets, Phys. Rev. B **108**, L180401 (2023).
[6] P. Rao, A. Mook, and J. Knolle, Tunable band topology and optical conductivity in altermagnets, Phys. Rev. B **110**, 024425 (2024).
[7] P. Das, V. Leeb, J. Knolle, and M. Knap, Realizing altermagnetism in Fermi-Hubbard models with ultracold atoms, Phys. Rev. Lett. **132**, 263402 (2024).
[8] J. Krempaský, L. Šmejkal, S. W. D'Souza, M. Hajlaoui, G. Springholz, K. Uhlířová, F. Alarab, P. C. Constantinou, V. Strocov, D. Usanov, *et al.*, Altermagnetic lifting of Kramers spin degeneracy, Nature (London) **626**, 517 (2024).
[9] O. Gomonay, V. P. Kravchuk, R. Jaeschke-Ubiergo, K. V. Yershov, T. Jungwirth, L. Šmejkal, J. v. d. Brink, and J. Sinova, Structure, control, and dynamics of altermagnetic textures, npj Spintron. **2**, 35 (2024).
[10] L. Bai, W. Feng, S. Liu, L. Šmejkal, Y. Mokrousov, and Y. Yao, Altermagnetism: Exploring new frontiers in magnetism and spintronics, Adv. Funct. Mater. **34**, 2409327 (2024).
[11] G. Yang, Z. Li, S. Yang, J. Li, H. Zheng, W. Zhu, Z. Pan, Y. Xu, S. Cao, W. Zhao, *et al.*, Three-dimensional mapping of the altermagnetic spin splitting in CrSb, Nat. Commun. **16**, 1442 (2025).
[12] S.-W. Cheong and F.-T. Huang, Altermagnetism classification, npj Quantum Mater. **10**, 38 (2025).
[13] S. D. Lundemo, F. S. Nogueira, and A. Sudbø, Quantum critical scaling of altermagnetism, Phys. Rev. B **111**, 214436 (2025).
[14] X.-J. Yi, Y. Mao, X. Lu, and Q.-F. Sun, Spin splitting Nernst effect in altermagnets, Phys. Rev. B **111**, 035423 (2025).
[15] C. Song, H. Bai, Z. Zhou, L. Han, H. Reichlova, J. H. Dil, J. Liu, X. Chen, and F. Pan, Altermagnets as a new class of functional materials, Nat. Rev. Mater. **10**, 473 (2025).
[16] J. Gondolf, A. Kreisel, M. Roig, Y. Yu, D. F. Agterberg, and B. M. Andersen, Local signatures of altermagnetism, Phys. Rev. B **111**, 174436 (2025).
[17] S. Iguchi, H. Kobayashi, Y. Ikemoto, T. Furukawa, H. Itoh, S. Iwai, T. Moriwaki, and T. Sasaki, Magneto-optical spectra of an organic antiferromagnet as a candidate for an altermagnet, Phys. Rev. Res. **7**, 033026 (2025).
[18] R. D. G. Betancourt, J. Zubáč, K. Geishendorf, P. Ritzinger, B. Růžičková, T. Kotte, J. Železný, K. Olejník, G. Springholz, B. Büchner, A. Thomas, K. Výborný, T. Jungwirth, H. Reichlová, and D. Kriegner, Anisotropic magnetoresistance in altermagnetic MnTe, npj Spintron. **2**, 45 (2024).
[19] R. Hoyer, P. P. Stavropoulos, A. Razpopov, R. Valentí, L. Šmejkal, and A. Mook, Altermagnetic splitting of magnons in hematite α-fe_2o_3, Phys. Rev. B **112**, 064425 (2025).
[20] V. Leeb, A. Mook, L. Šmejkal, and J. Knolle, Spontaneous formation of altermagnetism from orbital ordering, Phys. Rev. Lett. **132**, 236701 (2024).
[21] N. Kaushal and M. Franz, Altermagnetism in modified Lieb lattice Hubbard model, Phys. Rev. Lett. **135**, 156502 (2025).
[22] S. Sachdev, *Quantum Phase Transitions* (Cambridge University Press, Cambridge, 1999).
[23] T. Giamarchi, *Quantum Physics in One Dimension* (Oxford University Press, Oxford, 2004).
[24] G. D. Mahan, *Many Particle Physics* (Plenum Publishers, New York, 1990).
[25] G. Giuliani and G. Vignale, *Quantum Theory of the Electron Liquid* (Cambridge University Press, Cambridge, 2005).

[26] P. W. Phillips, L. Yeo, and E. W. Huang, Exact theory for superconductivity in a doped Mott insulator, Nat. Phys. **16**, 1175 (2020).
[27] Y. Hatsugai and M. Kohmoto, Exactly solvable model of correlated lattice electrons in any dimensions, J. Phys. Soc. Jpn. **61**, 2056 (1992).
[28] D. Lidsky, J. Shiraishi, Y. Hatsugai, and M. Kohmoto, Simple exactly solvable models of non-Fermi-liquids, Phys. Rev. B **57**, 1340 (1998).
[29] J. Zhao, L. Yeo, E. W. Huang, and P. W. Phillips, Thermodynamics of an exactly solvable model for superconductivity in a doped Mott insulator, Phys. Rev. B **105**, 184509 (2022).
[30] M. Zhao, W.-W. Yang, H.-G. Luo, and Y. Zhong, Friedel oscillation in non-Fermi liquid: Lesson from exactly solvable Hatsugai–Kohmoto model, J. Phys.: Condens. Matter **35**, 495603 (2023).
[31] D. Guerci, G. Sangiovanni, A. J. Millis, and M. Fabrizio, Electrical transport in the Hatsugai-Kohmoto model, Phys. Rev. B **111**, 075124 (2025).
[32] Y. Ma, J. Zhao, E. W. Huang, D. Kush, B. Bradlyn, and P. W. Phillips, Charge susceptibility and Kubo response in Hatsugai-Kohmoto-related models, Phys. Rev. B **112**, 045109 (2025).
[33] J. Zaanen, Carriers that count, Nat. Phys. **16**, 1171 (2020).
[34] M. Zhao, W.-W. Yang, and Y. Zhong, Hatsugai-Kohmoto models: Exactly solvable playground for Mottness and non-Fermi liquid, J. Phys.: Condens. Matter **37**, 183005 (2025).
[35] P. Mai, J. Zhao, G. Tenkila, N. A. Hackner, D. Kush, D. Pan, and P. W. Phillips, Twisting the Hubbard model into the momentum-mixing Hatsugai–Kohmoto model, Nat. Phys. **22**, 81 (2026)
[36] G. D. Mahan, *Many-Particle Physics*, 3rd ed. (Springer US, New York, NY, 2000).
[37] R. Kubo, Statistical-mechanical theory of irreversible processes. I. General theory and simple applications to magnetic and conduction problems, J. Phys. Soc. Jpn. **12**, 570 (1957).
[38] J. P. F. LeBlanc, A. E. Antipov, F. Becca, I. W. Bulik, G. K.-L. Chan, C.-M. Chung, Y. Deng, M. Ferrero, T. M. Henderson, C. A. Jiménez-Hoyos, *et al.* (Simons Collaboration on the Many-Electron Problem), Solutions of the two-dimensional Hubbard model: Benchmarks and results from a wide range of numerical algorithms, Phys. Rev. X **5**, 041041 (2015).
[39] I. M. Lifshitz, Anomalies of electron characteristics of a metal in the high pressure region, J. Exptl. Theoret. Phys. (U.S.S.R.) **38**, 1569 (1960) [Sov. Phys. JETP **11**, 1130 (1960)].
[40] G. E. Volovik, Topological Lifshitz transitions, Low Temp. Phys. **43**, 47 (2017).
[41] S. Blundell, *Magnetism in Condensed Matter*, Oxford Master Series in Condensed Matter Physics (Oxford University Press, Oxford, UK, 2001).
[42] T. A. Maier and S. Okamoto, Weak-coupling theory of neutron scattering as a probe of altermagnetism, Phys. Rev. B **108**, L100402 (2023).
[43] Q. Faure, D. Bounoua, V. Baledent, A. Gukasov, V. O. Garlea, A. Ribeiro, J. G. Rau, S. Petit, and P. McClarty, Altermagnetism revealed by polarized neutrons in MnF_2, arXiv:2509.07087.
[44] C. P. Slichter, *Principles of Magnetic Resonance*, 3rd ed. (Spinger, New York, NY, 1989).
[45] Y. J. Sun, F. Yang, and L. Q. Chen, Spin relaxation and transport behavior in d-wave altermagnetic systems, Phys. Rev. B **112**, 024412 (2025).
[46] K. Y. Povarov, J. Wosnitza, S. Rossler, M. Schmidt, A. A. Tsirlin, and S. A. Zvyagin, Low-energy magnons in the altermagnet α-MnTe, arXiv:2510.24376.
[47] J. Stenger, S. Inouye, A. P. Chikkatur, D. M. Stamper-Kurn, D. E. Pritchard, and W. Ketterle, Bragg spectroscopy of a Bose-Einstein condensate, Phys. Rev. Lett. **82**, 4569 (1999).
[48] A. A. Abrikosov, *Fundamentals of the Theory of Metals* (North-Holland, Amsterdam, 1998).
[49] A. Bácsi and B. Dóra, Source code and numerical data for the study "Interaction enhanced altermagnetism in the Hatsugai-Kohmoto model", Zenodo (2026), https://doi.org/10.5281/zenodo.20176677.